JOURNAL OF AGRICULTURAL AND FOOD CHEMISTRY
ARTICLE

J. Agric. Food Chem. 2010, 58, 563–569 563
DOI:10.1021/jf9028046

Differential Tissue Distribution of Sesaminol Triglucoside and Its Metabolites in Rats Fed with Lignan Glycosides from Sesame Meal with or without Nano/Submicrosizing

Chia-Ding Liao,[†,‡] Wei-Lun Hung,[†] Wen-Chien Lu,[†] Kuo-Ching Jan,[†] Daniel Yang-Chih Shih,[‡] An-I Yeh,[†] Chi-Tang Ho,[†,§] and Lucy Sun Hwang*[,†]

[†]Graduate Institute of Food Science and Technology, National Taiwan University, Taipei, Taiwan, [‡]Bureau of Food and Drug Analysis, Department of Health, Taipei, Taiwan, and [§]Department of Food Science, Rutgers University, 65 Dudley Road, New Brunswick, New Jersey 08901

Lignan glycosides are important functional compounds in sesame meal. In the present study, we investigated whether the tissue distribution of nano/submicrosized lignan glycosides from sesame meal (N-LGSM) differs from lignan glycosides from sesame meal (LGSM). LGSM was nano/submicrosized with 0.3 mm zirconia beads as the milling media. The average particle size of the 4% LGSM aqueous suspension reduced rapidly from approximately 2 μm to 200 nm after media milling at an agitation speed of 3600 rpm for 30 min. We examined the tissue distribution of sesaminol triglucoside (ST), the main component in LGSM, in Sprague-Dawley (SD) rats. The concentrations of ST were determined in various tissues and plasma within a 24 h period after oral administration of N-LGSM and LGSM (800 mg/kg of body weight). The results showed that higher concentrations of ST and its metabolites (sesaminol, sesaminol sulfate, and sesaminol glucuronide) were found in N-LGSM compared to those in LGSM in most tissues, especially liver and small intestine. Sesaminol glucuronide was the main metabolite in rats. After 3 h of oral administration, around 70% higher concentration of sesaminol glucuronide was found in N-LGSM compared to that in LGSM. This study clearly showed that LGSM is more bioavailable after nano/submicrosizing.

KEYWORDS: Sesame meal; sesaminol triglucoside; nanosuspension; tissue distribution; metabolites

INTRODUCTION

Sesame (*Sesamum indicum* L.) has been known as a traditional health food in East Asian countries. Sesame seed, composed of 50% lipid and 20% protein, is one of the important oilseed crops in the world (*1*, *2*). Lignans and lignan glycosides are important functional components in sesame. Lignan glycosides, existing mainly in the defatted sesame meal, are hydrophilic antioxidants. The major lignan glycosides found in sesame are sesaminol glucosides, pinoresinol glucosides, and sesamolinol glucosides (*3*, *4*). Several biological effects of these lignan glycosides have been studied. Sesame lignan compounds including sesaminol glucosides have been shown to inhibit lipid peroxidation as well as oxidative DNA damage in rat liver and kidney (*5*). Dietary defatted sesame flour containing 1% sesaminol glucoside has been reported to decrease susceptibility to oxidative stress in hypercholesterolemic rabbits (*6*). It was also reported that sesaminol glucosides have an antiinflammatory effect through inhibition on nuclear factor κB (NF-κB) and may be a useful agent for prevention of inflammatory disease such as Alzheimer's disease (*7*). In addition, it has been shown that sesaminol glucosides could inhibit azoxymethane- (AOM-) induced carcinogenesis in rat colon and suggested sesaminol glucosides as a possible chemopreventive agent (*8*). As a waste byproduct, sesame meal would be of added value if it could be used in the food industry.

Nanotechnology is expected to create innovation and play an important role in various biomedical applications. Due to the advantage of size effect and high surface reactivity of nanoparticles, nanotechnology is already used in pharmaceutical applications to increase the bioavailability of drugs (*9*−*15*). Size-dependent tissue distribution of nanoparticles was also found in the literature (*16*−*18*). However, there are only few reports on applications of nanotechnology in foods. The advantages and limitations of its use in the food industry are not yet fully understood. Several techniques have been applied to produce nanosuspensions, such as media milling and high-pressure homogenization (*11*−*13*, *19*). The specific physicochemical properties at the nanoscale are expected to result in increased reactivity with biological systems. Due to the smaller particle size and larger surface area, the biological effects and bioavailability of traditional foods may be higher after nanosizing. In our previous *in vitro* finding (*20*), we examined the intestinal epithelial membrane transport and absorption of lignan glycosides from sesame meal (LGSM) and nano/submicrosized LGSM (N-LGSM) using the Caco-2 human colonic cell line, a model simulating human intestinal absorption. After 4 h of transport experiment using the Caco-2 cell monolayer model, higher transport efficiency of sesaminol triglucoside (ST), which is the main component in

*To whom correspondence should be addressed (telephone, +886-2-23629984; fax, +886-2-33664113; e-mail, lshwang@ntu.edu.tw).

© 2009 American Chemical Society
Published on Web 12/16/2009

LGSM, was found after nano/submicrosizing. However, more information on absorption, distribution, metabolism, and excretion of food nanoparticles *in vivo* is needed.

The aim of this study was to investigate whether the tissue distribution of ST and its metabolites in N-LGSM differs from that in LGSM. This is the first report describing the biodistribution of nano/submicrosized sesame lignans. We want to investigate if the size reduction would enhance the absorption of LGSM in rats.

MATERIALS AND METHODS

Materials and Chemicals. Black sesame meal was supplied by Yuan-Shun Food Co. (Yun-Ling County, Taiwan). Sulfatase (type H-1), D-saccharic acid 1,4-lactone, and β-glucuronidase (type E-1) were obtained from Sigma-Aldrich (St. Louis, MO). Methanol (purity = 99.5%, HPLC grade) and *n*-hexane (purity = 98%) were purchased from Merck Co. (Darmstadt, Germany) and Tedia Co. (Fairfield, OH), respectively. Deionized water (Millipore Co., Bedford, MA) was used for all preparations.

Sesaminol triglucoside (ST) standard (purity = 99%, identified by nuclear magnetic resonance spectroscopy) and sesaminol standard (purity = 98%, identified by nuclear magnetic resonance spectroscopy) were extracted and purified from sesame meal in our own laboratory as reported previously (*21*). The chemical structures of ST and sesaminol are shown in **Figure 1**.

Animals. Sprague-Dawley (SD) rats (275 ± 25 g), supplied by BioLASCO Co. (Taipei, Taiwan), were used for tissue distribution study. First, the animals were acclimatized at a temperature of 20−22 °C and a relative humidity of 50−70% under a 12 h light/dark cycle for 1 week fed with AIN 93 M diet (Purina Mills, St. Louis, MO) and water ad libitum. The experimental protocol was approved by the National Laboratory Animal Center (Taipei, Taiwan).

Preparation of the Crude Extract of Lignan Glycosides. The method was adapted from Shyu et al. (*2*). Black sesame meal was extracted with *n*-hexane (1:10, g/mL) by stirring for 8 h at room temperature (two times). After removal of supernatant, the defatted sesame meal was collected and then extracted with 80% methanol (1:10, g/mL) by stirring for 8 h at room temperature (two times). This methanol extract was desolventized under reduced pressure to afford the crude extract of LGSM for the following experiments. The yield of LGSM from raw sesame meal was approximately 6%. LGSM contained 18.5% sesaminol triglucoside, an important bioactive compound in sesame meal.

Preparation of Nano/Submicrosuspension of Lignan Glycosides from Sesame Meal. The detailed method has been described in our recent publication (*20*). In brief, nano/submicrosized LGSM was produced by a media milling machine (MiniPur; Netzsch-Feinmahltechnik GmbH, Staufen, Germany) using a wet-milling process. It was performed using Yttria-stabilized zirconia beads with a diameter of 0.3 mm. Sixteen grams of LGSM powder was suspended in 400 mL of deionized water. The milling time was 30 min at the agitation speed of 3600 rpm. The suspension was agitated and recycled in the milling system by a pump. The bulk volume of milling medium was 140 mL. The process was performed at room temperature.

Particle Size and Morphology Determination. The detailed method has been described in a recent publication (*20*). In brief, dynamic light scattering measurements were performed using a light scattering particle size analyzer (Nanotrac 150; Microtrac Inc., Largo, FL). The size and morphology of N-LGSM were also studied by transmission electron microscopy (TEM; Model JSM-1200EX II; JEOL, Tokyo, Japan). Ten microliters of N-LGSM was added to 200 mesh carbon-coated copper grids (Electron Microspray Science, Hatfield, PA), and the excess liquid was drained off with a Whatman filter paper. Copper grids containing the sample as a dry film were placed on a TEM sample holder and observed at an accelerating voltage of 80 kV. A Sudan stain test was also performed using a 0.2% Sudan III (Sigma-Aldrich, St. Louis, MO) solution in 70% ethanol.

Tissue Distribution Studies. The method was adapted from Jan et al. (*21*, *22*) and Nardini et al. (*23*). LGSM or nano/submicrosized LGSM (N-LGSM) was administered via gastric gavage to two groups of rats (n = 15) for 4 days in three daily doses of 800 mg/kg body weight, a total of 2400 mg/kg body weight per day. Rats were anesthetized, using CO_2 as a carrier, at 1, 3, 6, 9, and 24 h (three rats were used for each time point) after the final tube feeding on the fourth day. Blood obtained by heart puncture was collected in heparin tubes, and plasma was subsequently prepared in centrifuge tubes by centrifuging at 1000*g* at 4 °C for 20 min. Heart, liver, spleen, lung, kidney, stomach, small intestine, cecum, colon, and rectum samples were collected after lightly rinsing with normal saline. Plasma and tissue samples were frozen at −80 °C until analysis.

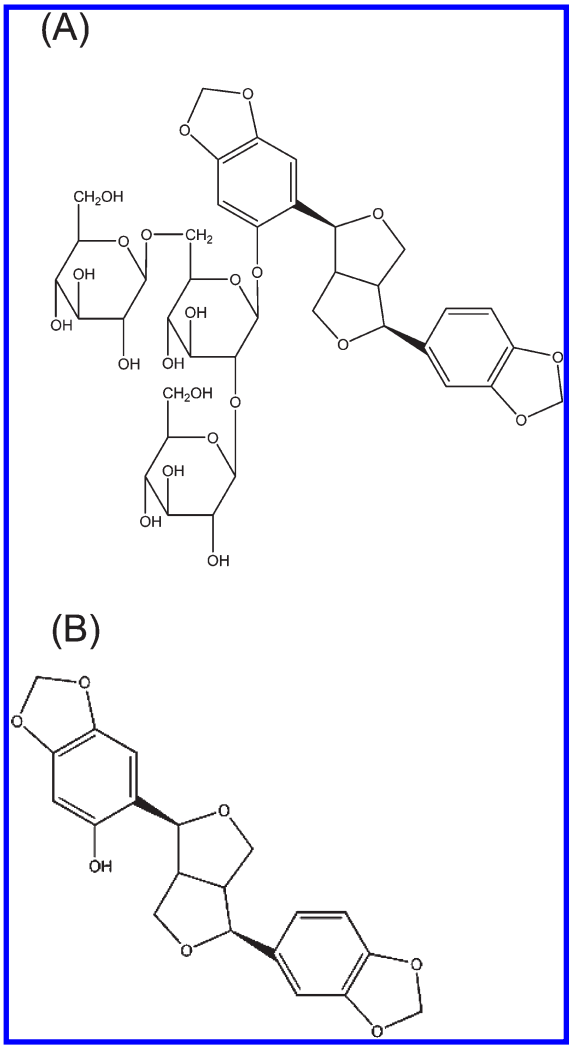

Figure 1. Chemical structures of (**A**) sesaminol triglucoside and (**B**) sesaminol.

Extraction. For extraction, rat tissues, weighted in 50 mL tubes, were homogenized by Polytron with normal saline. The homogenate was then mixed with acetonitrile (1:2, v/v) by a shaker for 30 min. The extract was centrifuged at 10000 rpm for 10 min at 4 °C. The supernatant was transferred to a clean tube and evaporated by nitrogen at 50 °C. Subsequently, the dried supernatant was dissolved with 1 mL of 0.1 N sodium acetate buffer (pH 5.0, with 200 mg/mL ascorbic acid) to obtain the tissue homogenate sample.

One hundred microliters of tissue homogenate sample or plasma was added with 50 μL of 0.1 N HCl and 250 μL of acetonitrile solution. The sample was then deproteinized by vortex mixing for 30 s. The deproteinized sample was centrifuged at 10000 rpm for 10 min at 4 °C. The supernatant was transferred to a clean tube and evaporated by nitrogen at 50 °C. Then the dried supernatant was dissolved with 1 mL of 0.1 N sodium acetate buffer (pH 5.0). Twenty microliters of sample was injected into the HPLC system for determination of sesaminol triglucoside and sesaminol.

Sulfatase type H-1 from Sigma-Aldrich also contains β-glucuronidase activity. The activity of β-glucuronidase can be totally inhibited by performing the enzymatic reaction in the presence of D-saccharic acid

1,4-lactone (*23*). For determination of sesaminol sulfate, 100 μL of tissue homogenate sample or plasma was added with 50 μL of sulfatase (1000 units/mL), 50 μL of D-saccharic acid 1,4-lactone (26 mM), and 50 μL of ascorbic acid (200 mg/mL) dissolved in 0.1 N sodium acetate buffer (pH 5.0). After being incubated in a water bath at 37 °C for 2 h, the hydrolyzed sample was added with 250 μL of acetonitrile and 50 μL of 0.1 N HCl. After vortex mixing for 30 s, the deproteinized sample was centrifuged at 10000 rpm for 10 min at 4 °C. The supernatant was transferred to a clean tube and evaporated by nitrogen at 50 °C. Then the dried supernatant was dissolved with 1 mL of 0.1 N sodium acetate buffer (pH 5.0). Twenty microliters of sample was injected into the HPLC system. This procedure allows the measurement of free plus sulfate conjugates of sesaminol. The amount of sulfates in plasma and tissue samples was calculated by subtracting the value of free, nonconjugated sesaminol content obtained with the above-reported procedure.

For determination of sesaminol glucuronide, 100 μL of tissue homogenate sample or plasma was added with 100 μL of β-glucuronidase (1000 units/mL) and 50 μL of ascorbic acid (200 mg/mL) dissolved in 0.1 N sodium acetate buffer (pH 5.0). After being incubated in a water bath at 37 °C for 2 h, the hydrolyzed sample was added with 250 μL of acetonitrile and 50 μL of 0.1 N HCl. After vortex mixing for 30 s, the deproteinized sample was centrifuged at 10000 rpm for 10 min at 4 °C. The supernatant was transferred to a clean tube and evaporated by nitrogen at 50 °C. Then the dried supernatant was dissolved with 1 mL of 0.1 N sodium acetate buffer (pH 5.0). Twenty microliters of sample was injected into the HPLC system. This procedure allows the measurement of free plus glucuronide conjugates of sesaminol. The amount of glucuronides in plasma and tissue samples was calculated by subtracting the value of free, nonconjugated sesaminol content obtained with the above-reported procedure.

Determination of Sesaminol Triglucoside and Its Metabolites. Concentrations of sesaminol triglucoside and its metabolites were determined by HPLC. The HPLC system consisted of a Shimadzu LC-10AT pump (Kyoto, Japan), a Hitachi L-4250 UV detector (Tokyo, Japan), and a Shimadzu SIL-10AF autosampler (Kyoto, Japan). Data acquisition was performed on a SISC program (Taipei, Taiwan). The Cosmosil 5C18-AR-II column (250 mm × 4.6 mm, 5 μm pore size; Nacalai, Kyoto, Japan) was maintained at 25 °C. The detector wavelength was 290 nm. The solvent system used was (A) water and (B) methanol. The linear gradient program used was the following: flow rate = 1.0 mL/min; 0−25 min, (A) 60% and (B) 40%; after 25 min, (A) 0% and (B) 100%. Injection volume was 20 μL.

Statistical Analysis. All data were reported as mean ± standard deviation (SD) for three replicates of each group. Sesaminol triglucoside, sesaminol, sesaminol sulfate, and sesaminol glucuronide concentrations were expressed in nanomoles per gram of tissue or nanomoles per milliliter of plasma. The statistical software Microsoft Office Excel (Microsoft Co., Redmond, WA) was used to perform the statistical analysis. Data were analyzed by Student's *t*-test analysis of variance, and the differences were considered to be statistically significant at $p < 0.05$.

RESULTS AND DISCUSSION

Preparation of Nano/Submicrosized Lignan Glycosides from Sesame Meal. We used a wet-milling machine to make the LGSM nano/submicrosuspension. Milling was performed using Yttria-stabilized zirconia balls with a diameter of 0.3 mm. Effective size reduction could be achieved by strong shear force and high frequency compression during milling. Results of dynamic light scattering measurements showed that the average particle size of LGSM was reduced from approximately 2 μm to 200 nm after 30 min of milling with a rotation speed of 3600 rpm. The TEM photograph also showed that the N-LGSM are nano/submicroparticles having particle size around 200 nm with spherical and homogeneous morphology. Interestingly, the possible formation of nanoemulsion droplets was found, which may be due to the presence of lipid and protein in LGSM and the high speed homogenization during the process of nanonization. The positive result of the Sudan stain test and the composition analysis of LGSM were reported in our recent publication (*20*).

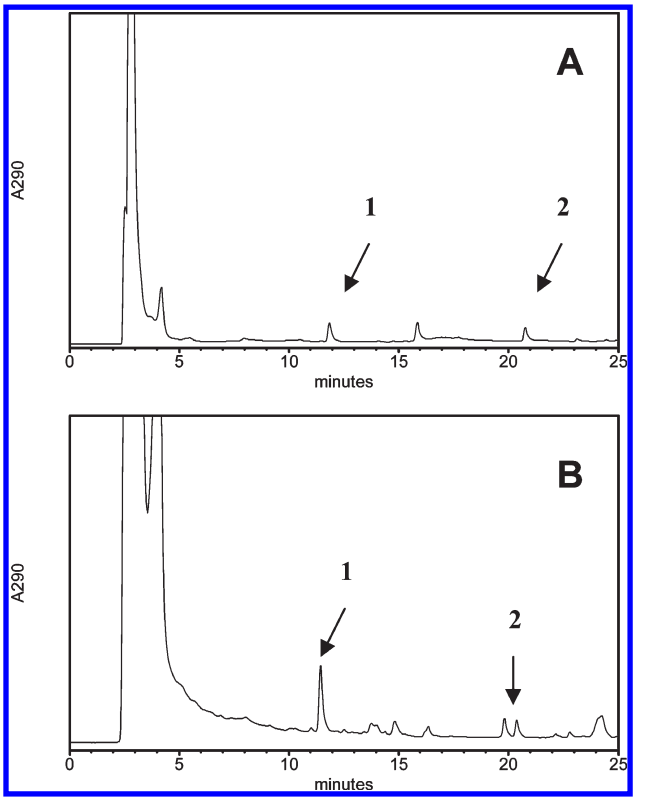

Figure 2. HPLC chromatograms of sesaminol triglucoside (ST) and sesaminol in (**A**) liver and (**B**) small intestine of rat collected at 6 h after oral administration of nano/submicrosized LGSM. Peaks: 1, sesaminol triglucoside; 2, sesaminol.

Organs Distribution of Nano/Submicrosized Lignan Glycosides from Sesame Meal. In this study, we analyzed the concentration of ST and its metabolites (sesaminol, sesaminol sulfate, and sesaminol glucuronide) to investigate the biodistribution in rats within 24 h after oral administration. A method of measuring ST, the main component in lignan glycosides from sesame meal, was developed. The determination of ST was performed using HPLC/UV for quantification. The method adapted from Jan et al. (*21*) has been used to analyze ST in various tissues. The maximum absorption wavelength (290 nm) of ST determined by a photodioarray detector was employed as the UV detecting wavelength in the following analysis. The linear gradient program of mixed solvents of water and methanol was used. The Cosmosil 5C18-AR-II column showed good performance in HPLC analyses. In addition, the quantitative method for determination of ST-conjugated metabolites (sulfate and glucuronide form) by HPLC was established in this study. While doing sulfate analysis, it is necessary to add D-saccharic acid 1,4-lactone as an inhibitor for β-glucuronidase. Because the commercial sulfatase (from *Helix pomatia*) has both activities of sulfatase and β-glucuronidase, it hydrolyzes not only sesaminol sulfate but also sesaminol glucuronide.

Typical HPLC chromatograms of sesaminol triglucoside and sesaminol in rat liver and small intestine collected after oral administration are shown in **Figure 2**. The retention time of sesaminol triglucoside and sesaminol was approximately 12 and 21 min, respectively. This analytical method was rapid and reliable. As shown in **Figure 3**, ST and its metabolites were widely distributed in organs. The concentration of ST in N-LGSM was higher in liver (**Figure 3C**) and kidney (**Figure 3F**), compared to that in plasma (**Figure 3A**), heart (**Figure 3B**), spleen (**Figure 3D**), and lung (**Figure 3E**). In organs, the concentrations of ST reached

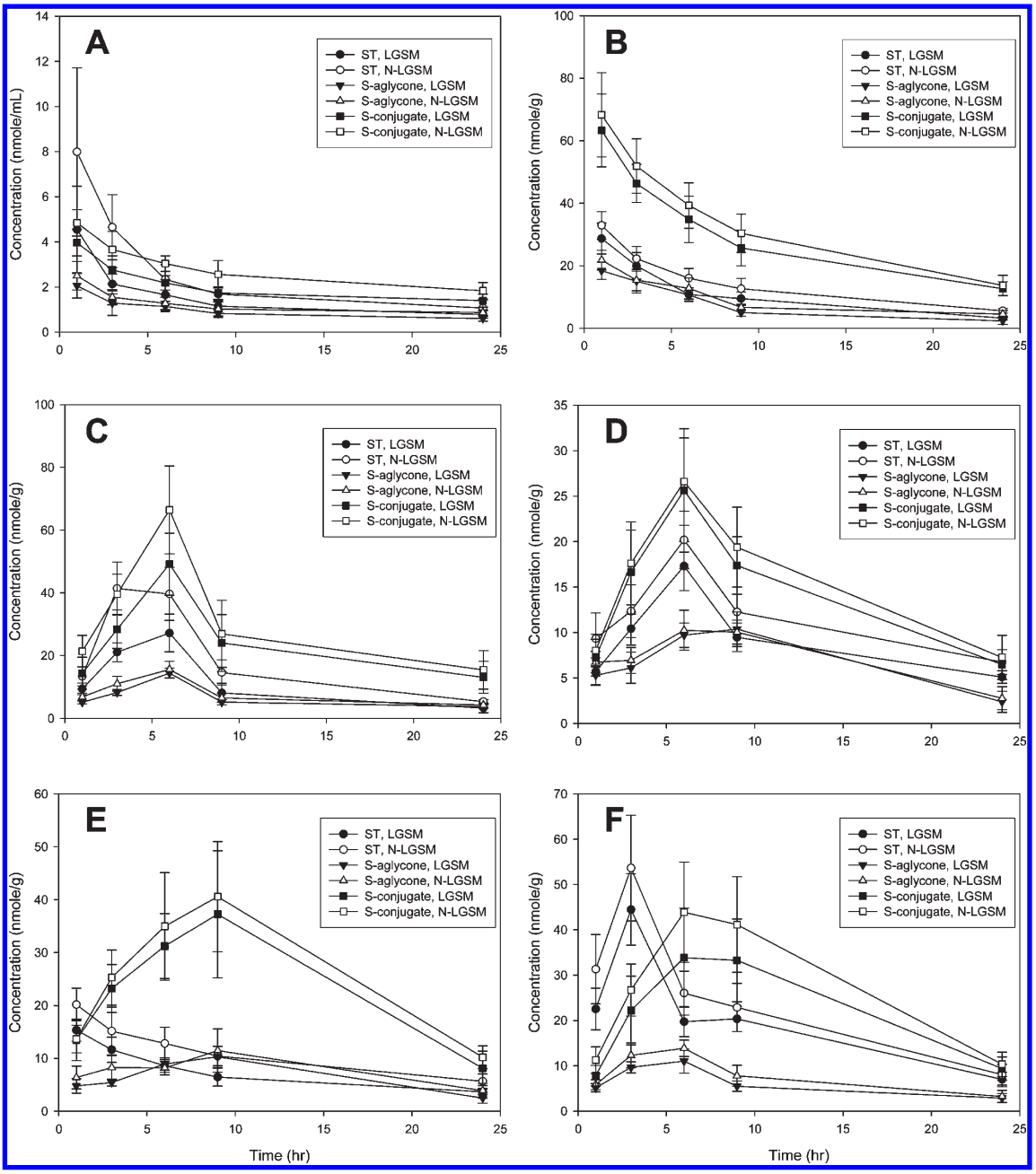

Figure 3. Concentration−time profiles for sesaminol triglucoside (ST) and its metabolites in (**A**) plasma, (**B**) heart, (**C**) liver, (**D**) spleen, (**E**) lung, and (**F**) kidney of rat after oral administration of LGSM and nano/submicrosized LGSM (N-LGSM). S = sesaminol. S-conjugate = *S*-sulfate + *S*-glucuronide.

maxima at 1−6 h after oral administration and decreased after 9 h. Conjugation reactions are considered to be the major detoxification processes in the body, but conjugation products may also be biologically active.

The liver is an important organ in the human body. It serves as a gatekeeper between the intestines and the general circulation. In this study, times to reach maximum concentration (T_{max}) of ST in N-LGSM and LGSM were 3 and 6 h, respectively, indicating smaller particles reached the liver more rapidly (**Figure 3C**). Enterohepatic circulation may occur faster in N-LGSM than in LGSM. The maximum concentrations (C_{max}) of ST in LGSM and N-LGSM were 27.17 ± 6.01 and 41.40 ± 8.42 nmol/g, respectively (**Table 1**). Higher concentrations of metabolites were also found in N-LGSM. Glucuronide seemed to predominate as ST metabolites *in vivo*. After 6 h of oral administration, around 50% higher concentration of sesaminol glucuronide was found in N-LGSM compared to that in LGSM. It had a significant difference in statistics ($p < 0.05$). The same trend was also found in heart, spleen, lung, kidney, and plasma. The C_{max} of ST and its metabolites in different organs was higher in N-LGSM than in LGSM.

Gastrointestinal Tract Distribution of Nano/Submicrosized Lignan Glycosides from Sesame Meal. Time-dependent changes of ST, sesaminol, and conjugated metabolite concentrations in rat stomach and intestines are shown in **Figure 4**. The concentrations of ST and its metabolites in large intestine (cecum, colon and rectum) were higher than those in stomach and small intestine and much higher than those in heart, liver, spleen, lung, and kidney. In the stomach and small intestine, the concentrations of ST and its metabolites reached maxima at 1 and 3 h, respectively, after oral administration and were rarely found after 24 h. In cecum, colon, and rectum, the concentrations of ST and its metabolites reached maxima at 6 and 9 h, respectively, after oral administration, longer than those in the stomach and small intestine.

Table 1. Concentrations of Sesaminol Triglucoside (ST) and Its Metabolites in Rat Liver at Each Time Point after Oral Administration of LGSM and Nano/Submicrosized LGSM (N-LGSM)[a]

	concn (nmol/g)							
	sesaminol triglucoside		sesaminol aglycon		sesaminol sulfate		sesaminol glucuronide	
time (h)	LGSM	N-LGSM	LGSM	N-LGSM	LGSM	N-LGSM	LGSM	N-LGSM
1	9.37 ± 1.87	13.36 ± 3.02	5.12 ± 0.51	6.80 ± 1.16	7.84 ± 3.08	11.68 ± 3.14	6.51 ± 2.02	9.71 ± 1.86[b]
3	21.06 ± 2.98	41.40 ± 8.42[b]	8.25 ± 0.96	11.03 ± 2.33[b]	14.54 ± 3.92	19.64 ± 2.89	13.82 ± 2.21	19.91 ± 3.53[b]
6	27.17 ± 6.01	39.64 ± 8.47[b]	14.43 ± 1.62	15.58 ± 2.60	23.02 ± 6.83	28.49 ± 9.84	26.14 ± 3.06	37.92 ± 4.16[b]
9	8.12 ± 3.05	14.59 ± 4.40	5.15 ± 0.86	6.50 ± 1.40	12.12 ± 5.01	14.41 ± 4.44	11.89 ± 4.04	12.50 ± 6.25
24	3.25 ± 1.48	5.32 ± 0.65[b]	3.74 ± 0.61	4.25 ± 0.65	6.77 ± 1.95	7.96 ± 2.36	6.30 ± 3.17	7.48 ± 3.80

[a] Data expressed as mean ± SD. Two groups (LGSM and N-LGSM) of rats (n = 15) were administered via gastric gavage for 4 days in three daily doses (800 mg/kg body weight). [b] Significantly different ($p < 0.05$) when compared with LGSM by Student's t-test.

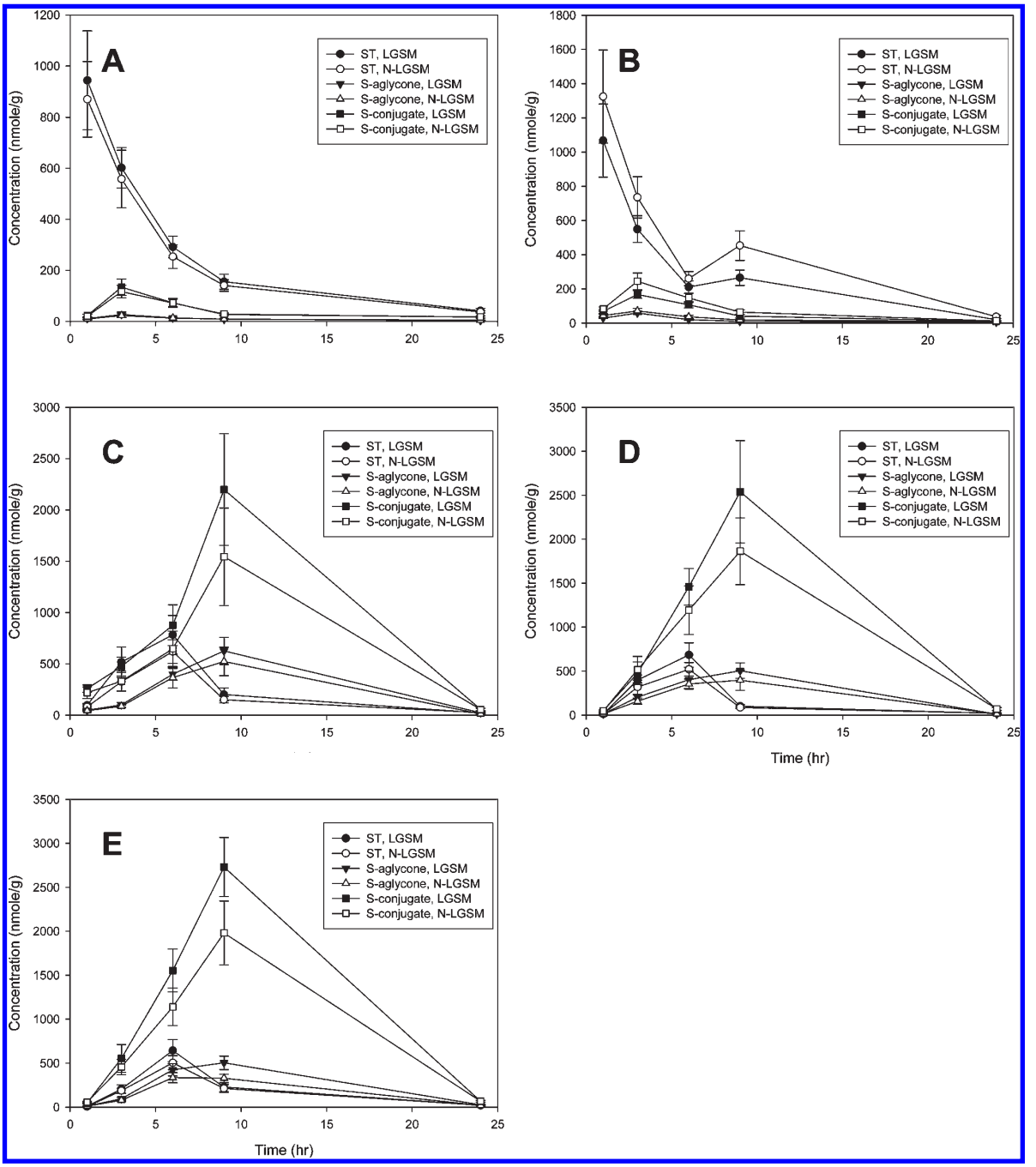

Figure 4. Concentration−time profiles for sesaminol triglucoside (ST) and its metabolites in (**A**) stomach, (**B**) small intestine, (**C**) cecum, (**D**) colon, and (**E**) rectum of rat after oral administration of LGSM and nano/submicrosized LGSM (N-LGSM). S = sesaminol. S-conjugate = *S*-sulfate + *S*-glucuronide.

Table 2. Concentrations of Sesaminol Triglucoside (ST) and Its Metabolites in Rat Small Intestine at Each Time Point after Oral Administration of LGSM and Nano/Submicrosized LGSM (N-LGSM)[a]

	concn (nmol/g)							
	sesaminol triglucoside		sesaminol aglycon		sesaminol sulfate		sesaminol glucuronide	
time (h)	LGSM	N-LGSM	LGSM	N-LGSM	LGSM	N-LGSM	LGSM	N-LGSM
1	1067.15 ± 213.49	1324.54 ± 271.98	29.14 ± 2.14	44.63 ± 7.97	24.93 ± 4.59	31.06 ± 5.13	43.28 ± 7.40	51.46 ± 7.18
3	549.07 ± 78.51	735.46 ± 120.55	59.19 ± 7.65	70.89 ± 15.39	69.81 ± 8.67	78.49 ± 12.20	97.83 ± 14.61	166.04 ± 36.35[b]
6	210.61 ± 36.20	260.11 ± 40.21	20.40 ± 4.81	38.66 ± 9.24[b]	28.03 ± 7.54	32.67 ± 8.54	79.37 ± 10.70	114.68 ± 18.26[b]
9	265.24 ± 44.36	453.22 ± 85.93[b]	9.84 ± 1.75	18.30 ± 3.23[b]	12.43 ± 3.28	15.21 ± 4.73	28.37 ± 7.57	49.35 ± 8.23[b]
24	20.67 ± 3.59	36.86 ± 8.47	6.09 ± 2.40	9.06 ± 3.56	4.74 ± 1.61	5.54 ± 0.85	6.16 ± 1.21	7.08 ± 1.62

[a] Two groups (LGSM and N-LGSM) of rats ($n = 15$) were administered via gastric gavage for 4 days in three daily doses (800 mg/kg body weight). [b] Data expressed as mean ± SD. Significantly different ($p < 0.05$) when compared with LGSM by Student's *t*-test.

In the biodistribution study, the most important information about absorption can be found from the results in the small intestine. The higher concentration of nutrient detected in the small intestine usually indicated better absorption. In this study, the concentrations of ST and its metabolites in small intestine were higher in N-LGSM than in LGSM. It seemed that the smaller particle size resulted in better absorption. Concentrations of ST and its metabolites in rat small intestine at each time point after oral administration are shown in **Table 2**. The T_{max} of ST and its metabolites in the small intestine was 1 and 3 h, respectively. Sesaminol glucuronide was the main metabolite in the small intestine. After 1 h of oral administration, ST concentrations in LGSM and N-LGSM were 1067.15 ± 231.49 and 1324.54 ± 271.98 nmol/g, respectively. After 3 h of oral administration, around 70% higher concentration of sesaminol glucuronide was found in N-LGSM compared to that in LGSM. Sesaminol glucuronide concentrations in LGSM and N-LGSM were 97.83 ± 14.61 and 166.04 ± 36.35 nmol/g, respectively. The difference is statistically significant ($p < 0.05$). Our results clearly showed that N-LGSM group had better small intestinal absorption.

The T_{max} of ST and its metabolites in colon was 6 and 9 h, respectively. Sesaminol glucuronide was the main metabolite in the colon. After 6 h of oral administration, ST concentrations in LGSM and N-LGSM were 683.67 ± 139.03 and 520.04 ± 76.66 nmol/g, respectively. After 9 h of oral administration, sesaminol glucuronide concentrations in LGSM and N-LGSM were 1490.49 ± 383.58 and 1217.26 ± 278.18 nmol/g, respectively. The opposite trend of tissue distribution was found in the large intestine compared to that in the small intestine. The large intestine receives the liquid residue after digestion and absorption. This residue consists mostly of water as well as materials that were not digested and absorbed. In this study, the lower level of ST in the large intestine was found in N-LGSM, indicating that the percentage of ST not absorbed was lower in N-LGSM compared to that in LGSM.

For particles with decreasing size, the ratio between the relative surface area and its volume will increase rapidly. Nano/submicrosized particles can be more reactive compared to larger particles because more surface area can interact with biological components of cells (*24*−*26*). Many reports have shown that the smaller the particle size, the higher the absorption efficiency. The bioavailability of regular carbendazim (7 μm) and its nanoparticle (280 nm) made by wet milling has been compared (*12*). It was found that the relative bioavailability of nanoparticle carbendazim versus regular carbendazim was 166%. Szentkuti (*27*) found that the smaller the particle, the faster the penetration action across the mucus barrier. Latex nanoparticles (14 and 415 nm) could penetrate the mucus gel layer in 2 and 30 min, respectively. Particles larger than 1 μm were unable to pass through the intestinal mucus barrier. In addition, size-dependent absorption of ^{125}I-labeled polystyrene latex particles was found by Jani et al. (*9*). Higher levels of polystyrene in intestine, stomach, liver, spleen, and urine were found in the group fed 100 nm particles than that fed 1 μm particles to rats, indicating the smaller the particle, the better the absorption. The trend was the same as the results we found in this study.

Our results demonstrated that in plasma, heart, liver, spleen, lung, kidney, and small intestine C_{max} of ST and its metabolites in N-LGSM was higher than that in LGSM. It clearly showed that LGSM is more bioavailable after nano/submicrosizing. Besides, shorter T_{max} of ST in liver and shorter T_{max} of sesaminol in spleen were found in N-LGSM compared to those in LGSM, indicating nano/submicroparticles might be transported and absorbed more rapidly and efficiently than microparticles in rats. The C_{max} of ST after oral administration to rats was in the following order: large intestine > small intestine > stomach > kidney ~ liver > heart > spleen ~ lung ~ plasma. In most organs, concentrations of ST-conjugated metabolites were higher than ST, indicating ST could be hydrolyzed and biotransformed to metabolites by intestinal enzymes and microflora. Glucuronide was the major metabolite, followed by sulfate. Conjugated metabolites (sulfate/glucuronide) were widely distributed in rat tissues, with the highest concentrations in intestines. It seemed that hydrolysis, sulfation, and glucuronidation of ST play an important role in intestines. The same trend was also shown in the literature (*21*).

The T_{max} of ST in small intestine, liver, and large intestine was 1, 3, and 6 h, respectively. ST was believed to pass through the small intestine and enter the large intestine, where it is hydrolyzed to aglycon by enterobacteria. A proportion of ST might be reabsorbed by the intestinal mucosa via the enterohepatic circulation. ST is mostly hydrolyzed to its aglycon by hydrolase, followed by conjugation to sulfate and glucuronide by sulfotransferase and UDP-glucuronosyltransferase before and during the process of intestinal absorption. Conjugated metabolites are transported into circulatory systems and excreted in urine. According to this study, the metabolites and metabolic pathways of LGSM and N-LGSM may not be different. However, at the same time point after oral administration, the concentrations of ST metabolites in N-LGSM differ significantly from those in LGSM. The higher absorption and bioavailability of nano/submicrosized LGSM may be attributed to the following factors: (a) smaller particle size and larger surface area provided by the fine particles, (b) increased mucosal permeability, and (c) improved intestinal absorption due to the formation of nanoemulsion droplets.

In our previous report (*20*), a similar trend was also found. In brief, we examined the intestinal epithelial membrane transport and absorption of LGSM and nano/submicrosized LGSM (N-LGSM) using the Caco-2 human colonic cell line, a model simulating human intestinal absorption. After 4 h of transport experiment using the Caco-2 cell monolayer model, higher

transport efficiency of sesaminol triglucoside (ST), which is the main component in LGSM, was found after nano/submicrosizing.

The results of this *in vivo* study confirm our previous *in vitro* finding that nano/submicronization may enhance the efficiency of small intestinal absorption. In addition, our study also provided a clear and helpful understanding of the tissue distribution of nano/submicrosized food components.

LITERATURE CITED

(1) Namiki, M. The chemistry and physiological functions of sesame. *Food Res. Int*. **1995**, *11*, 281–329.

(2) Shyu, Y. S.; Hwang, L. S. Antioxidative activity of the crude extract of lignan glycosides from unroasted Burma black sesame meal. *Food Res. Int*. **2002**, *236*, 357–365.

(3) Kuriyama, K. I.; Tsuchiya, K. Y.; Murui, T. Analysis of lignan glycosides in sesame seed by high pressure liquid chromatography. *Nippon Nogei Kagaku Kaishi* **1993**, *67*, 1693–1700.

(4) Katsuzaki, H.; Kawakishi, S.; Osawa, T. Sesaminol glucosides in sesame seeds. *Phytochemistry* **1994**, *35*, 773–776.

(5) Kang, M. H.; Natio, M.; Tsujihara, N.; Osawa, T. Sesamolin inhibits lipid peroxidation in rat liver and kidney. *J. Nutr*. **1998**, *128*, 1018–1022.

(6) Kang, M. H.; Kawai, Y.; Naito, M.; Osawa, T. Dietary defatted sesame flour decreases susceptibility to oxidative stress in hypercholesterolemic rabbits. *J. Nutr*. **1999**, *129*, 1885–1890.

(7) Lee, S. Y.; Son, D. J.; Lee, Y. K.; Lee, J. W.; Lee, H. J.; Yun, Y. W.; Ha, T. Y.; Hong, J. T. Inhibitory effect of sesaminol glucosides on lipopolysaccharide-induced NF-κB activation and target gene expression in cultured rat astrocytes. *Neurosci. Res*. **2006**, *56*, 204–212.

(8) Sheng, H. Q.; Hirose, Y.; Hata, K.; Zheng, Q.; Kuno, T.; Asano, N.; Yamada, Y.; Hara, A.; Osawa, T.; Mori, H. Modifying effect of dietary sesaminol glucosides on the formation of azoxymethane-induced premalignant lesions of rat colon. *Cancer Lett*. **2007**, *246*, 63–68.

(9) Jani, P.; Halbert, G. W.; Langridge, J.; Florence, A. T. Nanoparticle uptake by the rat gastrointestinal mucosa: quantitation and particle size dependency. *J. Pharm. Pharmacol*. **1990**, *42*, 821–826.

(10) Desai, M. P.; Labhasetwar, V.; Amidon, G. L.; Levy, R. J. Gastrointestinal uptake of biodegradable microparticles: effect of particle size. *Pharm. Res*. **1996**, *12*, 1838–1845.

(11) Jia, L.; Wong, H.; Cerna, C.; Weitman, S. D. Effect of nanonization on absorption of 301029: *ex vivo* and *in vivo* pharmacokinetic correlations determined by liquid chromatography/mass spectrometry. *Pharm. Res*. **2002**, *19*, 1092–1096.

(12) Jia, L.; Wong, H.; Wang, Y.; Garza, M.; Weitman, S. D. Carbendazim: disposition, cellular permeability, metabolite identification, and pharmacokinetic comparison with its nanoparticle. *J. Pharm. Sci*. **2003**, *92*, 161–172.

(13) Merisko-Liversidge, E.; McGurk, S. L.; Liversidge, G. G. Insulin nanoparticles: a novel formulation approach for poorly water soluble Zn-insulin. *Pharm. Res*. **2004**, *21*, 1545–1553.

(14) He, W. L.; Feng, Y.; Li, X. L.; Yang, X. E. Comparison of iron uptake from reduced iron powder and $FeSO_4$ using the Caco-2 cell model: effects of ascorbic acid, phytic acid, and pH. *J. Agric. Food Chem*. **2008**, *56*, 2637–2642.

(15) Zha, L. Y.; Xu, Z. R.; Wang, M. Q.; Gu, L. Y. Chromium nanoparticle exhibits higher absorption efficiency than chromium picolinate and chromium chloride in Caco-2 cell monolayers. *J. Anim. Physiol. Anim. Nutr*. **2008**, *92*, 131–140.

(16) Hillyer, J. F.; Albrecht, R. M. Gastrointestinal persorption and tissue distribution of differently sized colloidal gold nanoparticles. *J. Pharm. Sci*. **2003**, *90*, 1927–1936.

(17) De Jong, W. H.; Hagens, W. I.; Krystek, P.; Burger, M. C.; Sips, A. J. A. M.; Geertsma, R. E. Particle size-dependent organ distribution of gold nanoparticles after intravenous administration. *Biomaterials* **2008**, *29*, 1912–1919.

(18) Sonavane, G.; Tomoda, K.; Makino, K. Biodistribution of colloidal gold nanoparticles after intravenous administration: effect of particle size. *Colloids Surf., B* **2008**, *66*, 274–280.

(19) Gao, L.; Zhang, D.; Chen, M.; Duan, C.; Dai, W.; Jia, L.; Zhao, W. Studies on pharmacokinetics and tissue distribution of oridonin nanosuspensions. *Int. J. Pharm*. **2008**, *355*, 321–327.

(20) Liao, C. D.; Hung, W. L.; Jan, K. C.; Yeh, A. I.; Ho, C. T.; Hwang, L. S. Nano/sub-microsized lignan glycosides from sesame meal exhibit higher transport and absorption efficiency in Caco-2 cell monolayer. *Food Chem*. **2010**, *119*, 896–902.

(21) Jan, K. C.; Hwang, L. S.; Ho, C. T. Tissue distribution and elimination of sesaminol triglucoside and its metabolites in rat. *Mol. Nutr. Food Res*. **2009**, *53*, 815–825.

(22) Jan, K. C.; Ho, C. T.; Hwang, L. S. Bioavailability and tissue distribution of sesamol in rat. *J. Agric. Food Chem*. **2008**, *56*, 7032–7037.

(23) Nardini, M.; Natella, F.; Saccini, C.; Ghiselli, A. Phenolic acids from beer are absorbed and extensively metabolized in humans. *J. Nutr. Biochem*. **2006**, *17*, 14–22.

(24) Brown, D. M.; Wilson, M. R.; MacNee, W.; Stone, V.; Donaldson, K. Size-dependent proinflammatory effects of ultrafine polystyrene particles: a role for surface area and oxidative stress in the enhanced activity of ultrafines. *Toxicol. Appl. Pharmacol*. **2001**, *3*, 191–199.

(25) Oberdorster, G. Pulmonary effects of inhaled ultrafine particles. *Int. Arch. Occup. Environ. Health* **2001**, *74*, 1–8.

(26) Hagens, W. I.; Oomen, A. G.; Jong, W. H; Cassee, F. R.; Sips, A. J. A. M. What do we (need to) know about the kinetic properties of nanoparticles in the body? *Regul. Toxicol. Pharmacol*. **2007**, *49*, 217–229.

(27) Szentkuti, L. Light microscopical observations on luminally administered dyes, dextrans, nanospheres and microspheres in the preepithelial mucus gel layer of the rat distal colon. *J. Controlled Release* **1997**, *46*, 233–242.

Received for review August 11, 2009. Revised manuscript received November 23, 2009. Accepted November 27, 2009. This study was supported by research grant DOH97-TD-F-113 from the Department of Health, Taiwan.